THE BELL SYSTEM TECHNICAL JOURNAL
Vol. 59, No. 6, July–August 1980
*Printed in U.S.A.*

# Propagation Characteristics of Double-Mode Fibers

By L. G. COHEN, W. L. MAMMEL, C. LIN, and W. G. FRENCH

(Manuscript received January 21, 1980)

*We study propagation characteristics of double-mode fibers by measuring group delay differences of time-resolved discrete pulses of the LP(01) and LP(11) modes as a function of wavelength in the 1.06- to 1.6-μm region. The technique has been used to make the first measurements of zero intermodal dispersion in the zero material dispersion region of graded-index double-mode fiberguides that can have larger diameters than standard single-mode fibers. The results can also be used to deduce information about the fiber's refractive-index profile, such as Δ, the normalized peak refractive index difference.*

## I. INTRODUCTION

This paper describes transmission characteristics of double-mode fiberguides which can have larger diameters than single-mode fibers without sacrificing bandwidth. Wide bandwidths are achieved in double-mode fibers because there is a wavelength at which the group delays are the same for their two propagating modes.

The normalized frequency parameter, $V$, can be used to determine the number of modes in a fiberguide. When $V < V_{co} = 2.41\sqrt{1 + (2/g)}$, then only one mode,[1] designated LP(01),[2] propagates in a guide with a graded refractive-index profile described by $n = n_0\sqrt{1 - 2\Delta(r/a)^g}$. Since $V = (2\pi a/\lambda)\sqrt{2n\,\Delta n}$, it is evident that the core diameter, $2a$, and the core-to-cladding index difference, $\Delta n = n(0) - n(a)$, may be varied over a wide range while still maintaining single-mode operation.

However, when $V$ is significantly smaller than the cut-off value, $V_{co}$, the field propagating in the fiber becomes loosely guided and transmission losses increase due to bending and cladding imperfections. To minimize material dispersion effects, bending losses, and splicing difficulties, single-mode fibers should be designed with $V \approx V_{co}$ at a

wavelength as close as possible to a system carrier wavelength in the $\lambda = 1.3$-$\mu$m region.[3,4] This is achieved by designing core diameters to be about 15 $\mu$m and by having small index differences ($\Delta n \approx 0.0015$) between the core and cladding. Single-mode fibers designed for the 0.8-$\mu$m region have somewhat smaller core diameters that are typically 10 $\mu$m.[5]

Double-mode fibers could be used as an alternative to single-mode fibers if the group velocities of its two propagating modes were equalized at a system wavelength in the 1.3-$\mu$m region[6] or in the 0.8-$\mu$m region.[7] Then intermodal dispersion would be zero in waveguides with larger diameters than single-mode fibers. However, practical systems applications would require precise double-mode profile control since the zero double-modal dispersion wavelength depends on the shape of the profile.

The remainder of this paper describes a technique for determining the wavelength at which intermodal dispersion becomes zero in double-mode fibers. These are the first results reported in the 1.3-$\mu$m wavelength region where material dispersion effects are also very small. The technique can also be used to deduce the wavelength at which a single-mode fiber becomes double-moded as well as physical properties of the fiber such as its effective $g$ and $\Delta n$.

Measured results are compared to theoretical predictions based on exact numerical solutions for LP(01) and LP(11) propagating modes of the scalar differential wave equations for the electromagnetic fields. The numerical analysis includes the effect of dips in the refractive-index profile which occur at the center of the fiber core.

## II. THEORETICAL RESULTS

Figure 1 shows intermodal propagation characteristics of double-mode fibers with two different power law refractive-index profiles. Normalized modal group delays $\bar{\tau}$, defined by $\tau = \tau_0(1 + \Delta\bar{\tau})$, are plotted versus $V$-number for values ranging from about 2 to 6. These results were obtained from exact numerical solutions for propagating modes of the scalar differential wave equations for the electromagnetic fields. The horizontal dashed lines in the figures correspond to the time delay, $\tau_0/L$, for a plane wave propagating in a medium with the peak fiber core refractive-index, $n$. The two solid curves in each figure represent delay characteristics for LP(01) and LP(11) modes. The single-mode limit for a fiber occurs at the cut-off $V$-number for the LP(11) mode which is $V_{co} = 2.41$ for step-index fibers (Fig. 1a). Only two modes propagate for $V$-numbers to the left of the dashed vertical line where the LP(21) mode becomes cut off.

Zero intermodal dispersion occurs at the intersection point of the modal delay curves. Theoretical results, to be given in more detail in

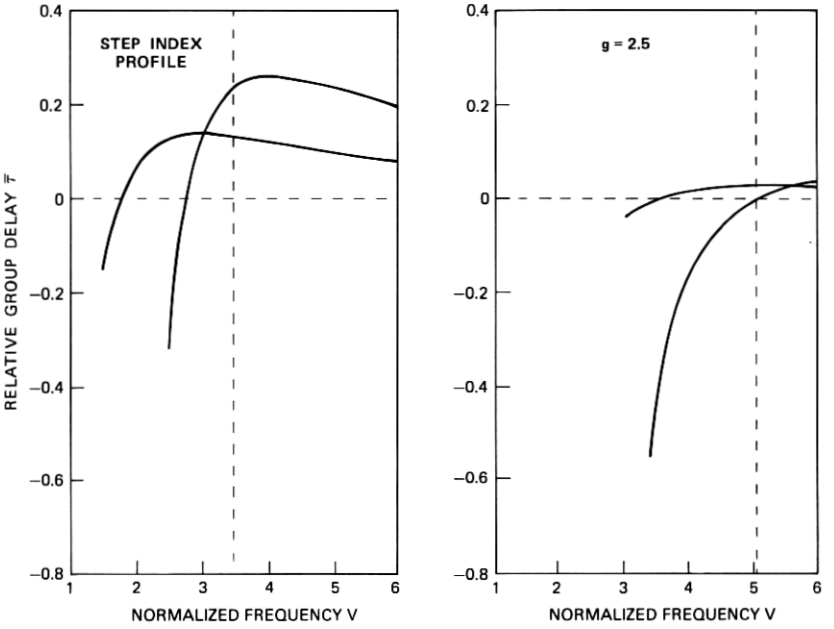


Fig. 1—Normalized group delays, $\bar{\tau}$ defined by $\tau = \tau_0(1 + \Delta\ \bar{\tau})$, vs normalized frequency, $V$, for LP(01) and LP(11) modes in fibers having step ($g = \infty$) and graded ($g = 2.5$) refractive-index profiles. The horizontal dashed lines in the figures correspond to the time delay, $\tau_0/L$, for a plane wave propagating in a medium with the peak core refractive-index, $n$. The vertical dashed lines indicate the cut-off $V$-number for the third propagating mode.

separate papers,[8,9] show that this point is almost entirely dependent upon the fiber's refractive-index profile shape. The equalization $V$-number is 3 for step-index fibers. Figure 1b applies to fibers with $g = 2.5$ profiles and shows the advantage of using graded-index double-mode fibers. The cut-off $V$-number is $V_{co} = 3.34$ for single-mode operation and the double-mode regime corresponds to $V < 5$. However, in practice, double-mode operation can be extended to $V$-values 10 to 20 percent higher than the third mode cut-off where the LP(21) mode is still very lossy due to the finite cladding thickness. Zero LP(01)-LP(11) intermodal dispersion in $g = 2.5$ fibers occurs when $V = 5.5$, which is almost two times larger than $V_{co}$ for single-mode operation and the equalization $V$-number for step-index fibers. This theoretical result implies that double-mode fibers with zero modal dispersion can be fabricated with core diameters that are twice as large as for single-mode fibers with step-index profiles.

Fibers fabricated for this study were made by the modified chemical vapor deposition (MCVD) technique.[1] Their cores consisted of $GeO_2$-doped silica and the cladding of pure silica. For a fiber with intentional index-grading, the core was deposited in several layers with different

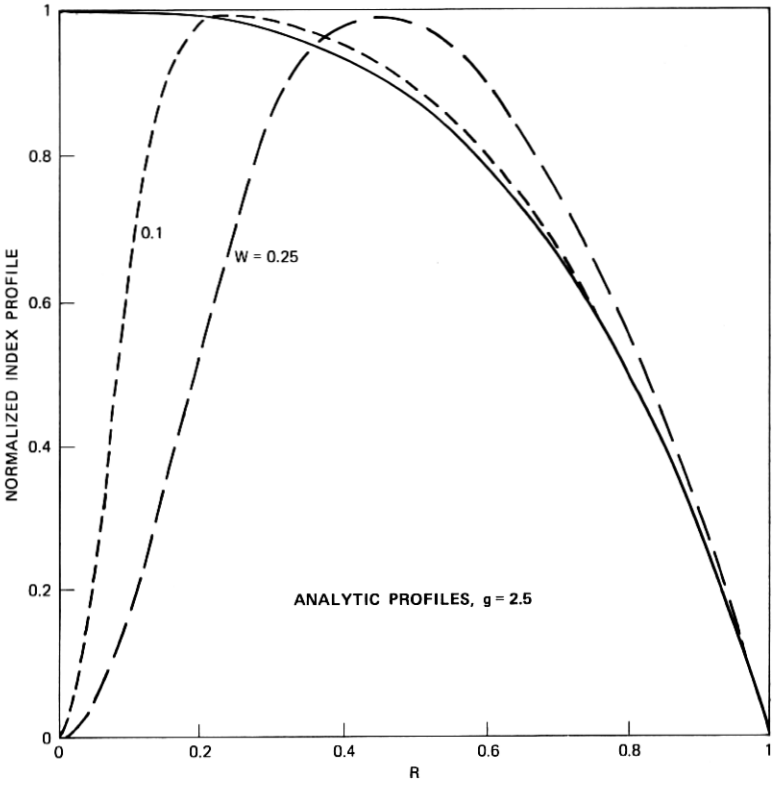


Fig. 2—Profiles of refractive-index vs radius, which are representative of fibers used in this study. The rms width, $w$, of the central index depression was about 25 percent of the core radius. Its depth, $d$, varied from about 50 to 100 percent of the maximum core radius.

$GeO_2$ concentrations. For the step-index fiber, the core composition was kept constant for each layer, but diffusion and/or dopant vaporization yielded some unintentional profile grading. Vaporization from the innermost layer caused refractive-index dips at the center of the core of each type of fiber. Figure 2 shows analytic profiles, with $g = 2.5$, of refractive index versus radius which are representative of fibers used in this study. The normalized profiles in Fig. 2 are given by $1 - N(r)$,

$$N(r) = \frac{r^g + d \cdot \exp(-(r/w)^2)(1 - r^g) - b}{1 - b}, \tag{1}$$

where $b$ is chosen so that the minimum of $N(r)$ is zero. The rms width, $w$, of the central index depression was about 25 percent of the core radius. Its depth, $d$, varied from about 50 to 100 percent of the maximum core index.

Figure 3 shows results of numerical studies to determine the effects of central refractive-index dips within power law $g$ profiles on the propagation characteristics of double-mode fibers. The group of three curves on the left show $g$ plotted versus the LP(11) cut-off $V$-number for single-mode operation. The solid curve applies to profiles without dips. Note that $g$ decreases from 8.0 to 2.5 as $V_{co}$ increases from 2.7 to 3.3. The dashed curves show the effect of a 100-percent deep index dip whose width is 10 percent of the core radius and the (—·—) curves show the effect of a 100-percent dip whose width is 25 percent of the core radius. These dips tend to increase the width of the propagating fields. A fiber without a dip having zero modal dispersion at $V = 4$ has a larger $g$ than a fiber with a dip which has zero modal dispersion at $V = 4$. This makes the effective profile $g$ seem larger than the fabricated $g$.

The group of three curves on the right of Fig. 3 show how refractive-index dips affect double-mode operation by reducing the $V$-numbers

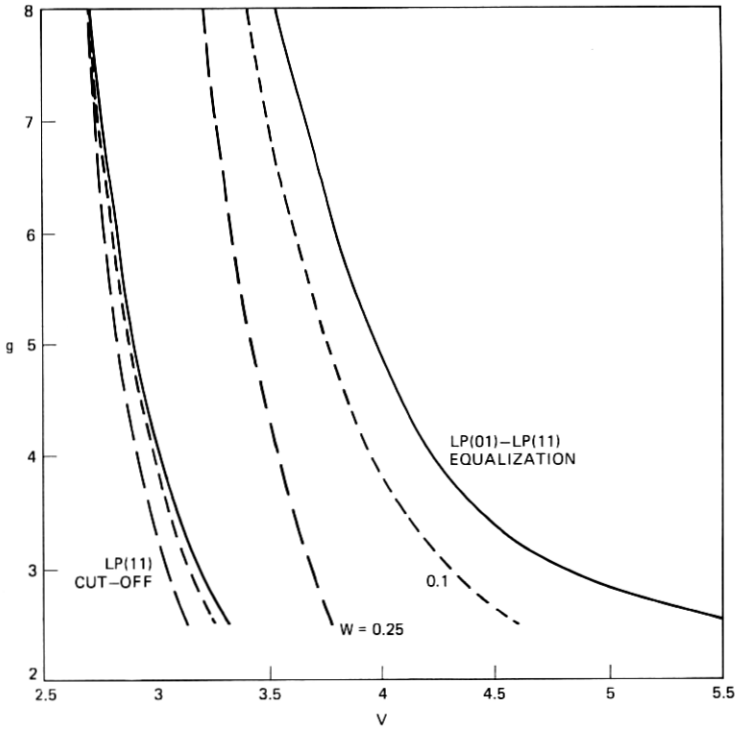


Fig. 3—Power law profile-$g$ vs $V$-number. The solid curves apply to profiles without dips. Data shown as (——) apply to profiles with $w = 1$, $d = 1$. Data shown as (—·—) apply to profiles with $w = 0.25$, $d = 1$. The group of three curves on the right are plotted vs the $V$-number for zero double-modal dispersion.

at which LP(01) and LP(11) modes are equalized. Note that the effect on double-mode operation is substantially greater than on single-mode operation. But again the dips make the effective profile $g$ appear larger than the fabricated $g$ values. For example, a 25-percent wide, 100-percent deep dip makes a fabricated profile $g$ of 2.5 act like an undistorted profile with $g = 5$. This indicates that the effect of the profile dip could be partially compensated for by a fabricated profile with $g < 2.5$.

When intermodal dispersion between LP(01) and LP(11) modes is zero, the fiber dispersion is due to intramodal material and waveguide effects for each of these modes. These effects are illustrated in Fig. 4, which is a plot of the dimensionless dispersion coefficient $D$ versus $V$-number, for the parameters listed, where $D$ is defined by the equation

$$\frac{d\tau}{d\lambda} = \frac{Ln_0}{c\lambda}\Delta D. \tag{2}$$

The effects of material and waveguide dispersion are interrelated, and the total chromatic dispersion is the sum of the standard material dispersion common to all modes and waveguide dispersion that in-

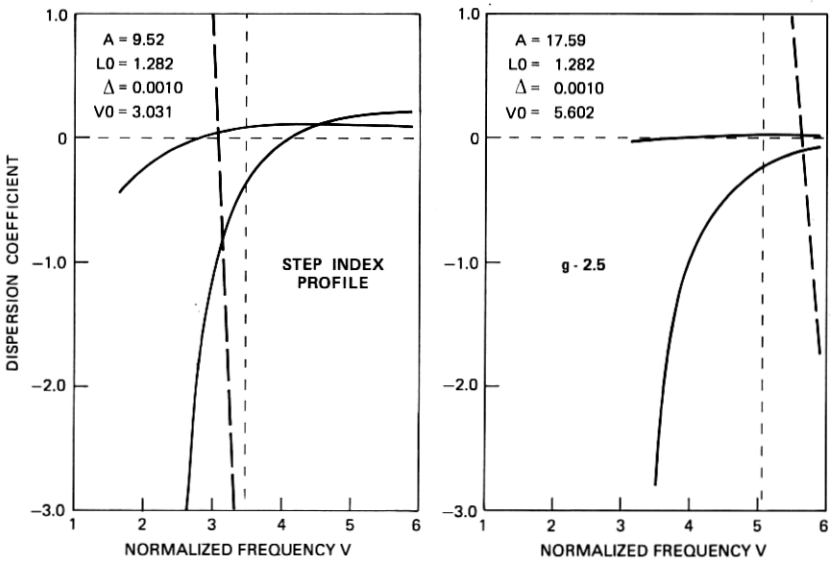


Fig. 4—Dimensionless dispersion coefficient $D$ vs $V$ for fibers with $g = \infty$ and $g = 2.5$. $D$ can be converted to units of ps/Km-nm through $(n_0/c\lambda)\Delta(\delta\lambda)D$. Material dispersion effects are illustrated by (——) data for $\Delta = 0.001$. The solid curves show waveguide dispersion effects for LP(01) and LP(11) modes. The fiber parameters $a$, $\Delta$, $V_0$ were calculated to make the zero double-modal dispersion wavelength, $\lambda_0$, equal to the zero material dispersion wavelength, 1.282 $\mu$m.

cludes material effects. In Fig. 4, the (—·—) curve shows the material dispersion coefficient, $D_m$ versus $V$. The solid curves show the waveguide dispersion coefficient, including material effects, for the LP(01) and LP(11) modes. The parameters are chosen so the zero material dispersion wavelength coincides with the zero intermodal dispersion wavelength. For germania-doped silica with $\Delta = 0.001$, the material dispersion is zero at $\lambda_0 = 1.282$ $\mu$m. This leaves the core radius $a$ to be chosen so the $V$-number for zero material dispersion coincides with the $V$-number for zero intermodal dispersion. For example, fibers with $g = 2.5$ profiles have zero intermodal and material dispersion at $\lambda_0 = 1.282$ $\mu$m if their index difference is $\Delta = 0.001$ within a core radius $a = 17.6$ $\mu$m. The dimensionless dispersion coefficient $D$ can be converted to pulse-broadening in ps/Km-nm by $3.76D$ ps/Km-nm, through $(n_0/c\lambda)\,\Delta(\delta\lambda)D$, with $n_0 = 1.45$, $c = 3 \times 10^5$ Km/s, $\lambda = 1.282$ $\mu$m, and with $(\delta\lambda)$ being the spectral bandwidth of the source in nautical miles. Therefore, waveguide dispersion effects, illustrated in Fig. 4, should cause less than 0.5 ps/Km-nm pulse broadening at the zero intermodal dispersion wavelength for double-mode fibers.

## III. EXPERIMENTAL RESULTS

Time-domain pulse-delay measurements were made with the Universal Fiber-Optic (UFO) measurement system described previously.[10] The optical source provides subnanosecond pulses at 1.06 $\mu$m and at any wavelength within the 1.1- to 1.6-$\mu$m spectral range. Transmission data are automatically acquired and processed by a microcomputer graphics terminal, which is now an integral part of the measurement system.

Transmission measurement results in Fig. 5 show that LP(01) and LP(11) modes can be time-resolved and verify that zero modal dispersion occurred in a double-mode fiber which was 500 meters long and had a graded refractive-index profile with an effective $g \approx 3$. Impulse responses are displayed on a 200-picosecond/div horizontal time scale for six wavelengths. The two modes in the fiber propagate as distinct pulses whose relative peak amplitudes could be changed by varying the input beam launching conditions. At $\lambda = 1.125$ $\mu$m, the first (least delayed) peak represented power propagating in the LP(01) mode because it was associated with a nearly Gaussian far-field radiation pattern. The second peak was associated with the LP(11) mode which has a doubly peaked, far-field radiation pattern. LP(01) to LP(11) modal dispersion characteristics are determined by measuring the intermodal group delay differences between the pulse peaks. Note that, as the wavelength increases, the time delay between peaks decreases until the pulses coalesce into a single narrow pulse at $g = 1.24$ $\mu$m wavelength

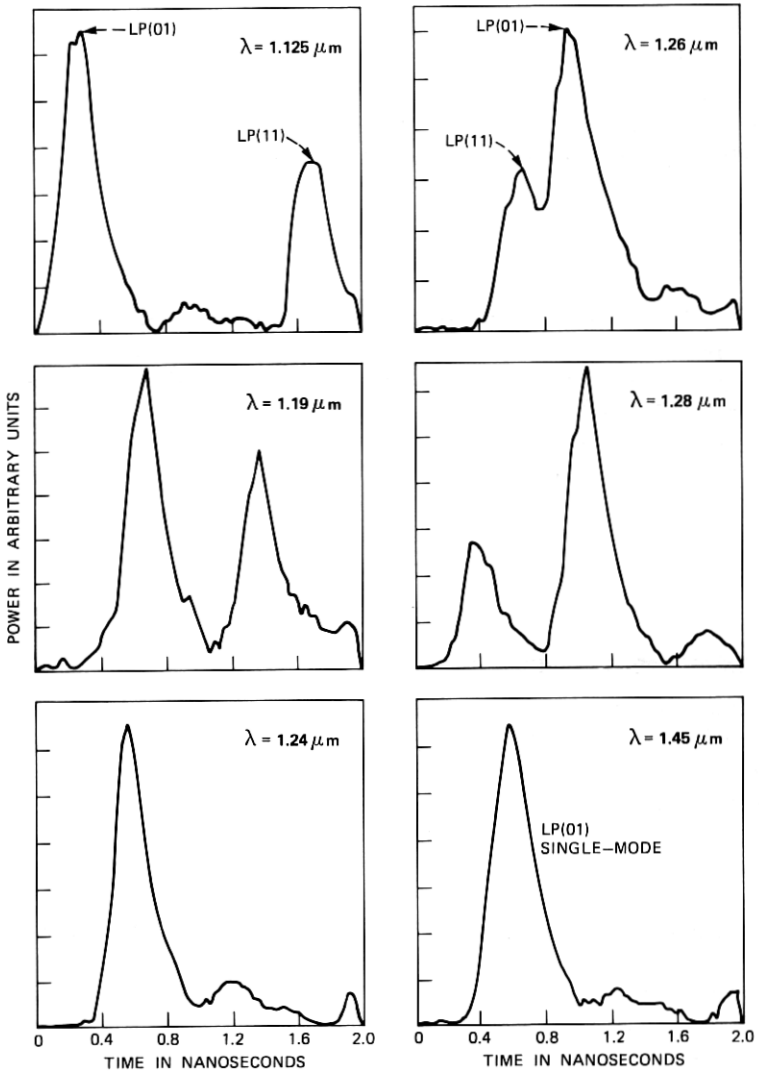


Fig. 5—Impulse responses are displayed on a 0.2 ns/div horizontal time scale for six wavelengths in a 0.5-Km-long graded-index fiber with an effective $g \approx 3$. Zero double-modal dispersion occurs at $\lambda = 1.24$ μm. The fiber is single-mode at $\lambda = 1.45$ μm because the LP(11) mode is cut off.

where the fiber $V$-number is $V = (2\pi a/\lambda)\sqrt{2n\,\Delta n} \approx 4.25$. For wavelengths longer than $\lambda = 1.24$ μm, the LP(11) mode is delayed less than the LP(01) mode, and the modal pulses become further separated as the wavelength increases to 1.28 μm. Finally, at $\lambda = 1.45$ μm, the LP(11) mode is cut off and the fiber is single-mode. Note that the double-

mode fiber response at $\lambda = 1.24$ $\mu$m is no more dispersive than the single-mode response at $\lambda = 1.45$ $\mu$m.

Figure 6 summarizes results from several different double-mode fibers. The intermodal group delay difference between the LP(01) and LP(11) modes is plotted versus $V$-number. Zero intermodal dispersion occurs when the curves intersect the horizontal axis. The solid theoretical delay curve, $S$, applies to step-index profiles with $\Delta n = 0.016$. The maximum lag time of the LP(11) mode behind the LP(01) mode is $\delta\tau \approx 500\ \Delta n$ ns/Km and can be used to estimate $\Delta n$ in step-index double-mode fibers. This enabled us to deduce that $\Delta n = 0.016$ and 0.010 in fabricated step-index fibers S-1 and S-2, respectively.

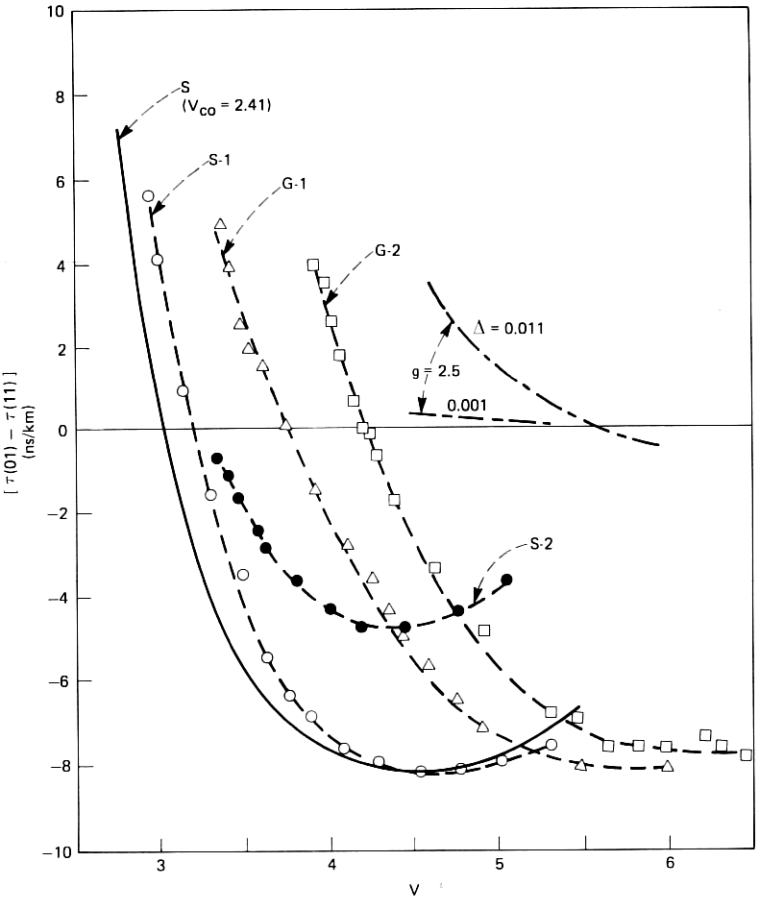


Fig. 6—Intermodal time delay differences $\delta\tau = (\tau(01) - \tau(11))$ vs $V$-number for double-mode fibers. Curve $S$ shows calculated results for a step-index fiber. Curves $S$-1, $S$-2 are results for fabricated fibers with nearly step-index profiles. Curves $G$-1, $G$-2 correspond to fibers with intentional index grading. The (—·—) delay curves were calculated for $g = 2.5$ profiles which are nearly optimal for double-mode operation.

In general, the relative delay between LP(01) and LP(11) modes is described by $\delta\tau = (L/c)(\bar{\tau}(11) - \bar{\tau}(01))\,\Delta n$. As shown in Fig. 1, $\bar{\tau}$ is a function of $g$ and $V$ and the maximum value of $\bar{\tau}(11) - \bar{\tau}(01) = T$ decreases as $g$ is decreased from $g = \infty$ to $g = 2$. However, for profiles with large index dips, $T$ is constant with respect to $g$. This phenomenon is illustrated in Fig. 7e which plots $T$ vs $g$ for profiles with dips with various depths, $d$, and rms widths, $w$. Note that $T \approx 0.155$ for profiles with 100-percent deep dips ($d = 1$) whose widths are 25 percent of the core radius ($w = 0.25$). This explains why the maximum $\delta\tau$ in Fig. 6 is nearly the same for fibers S-1, G-1, and G-2, which had approximately the same $\Delta n$ but different effective $g$-profile exponents with deep and wide dips.

Fibers G-1 and G-2 were fabricated with intentional index grading,

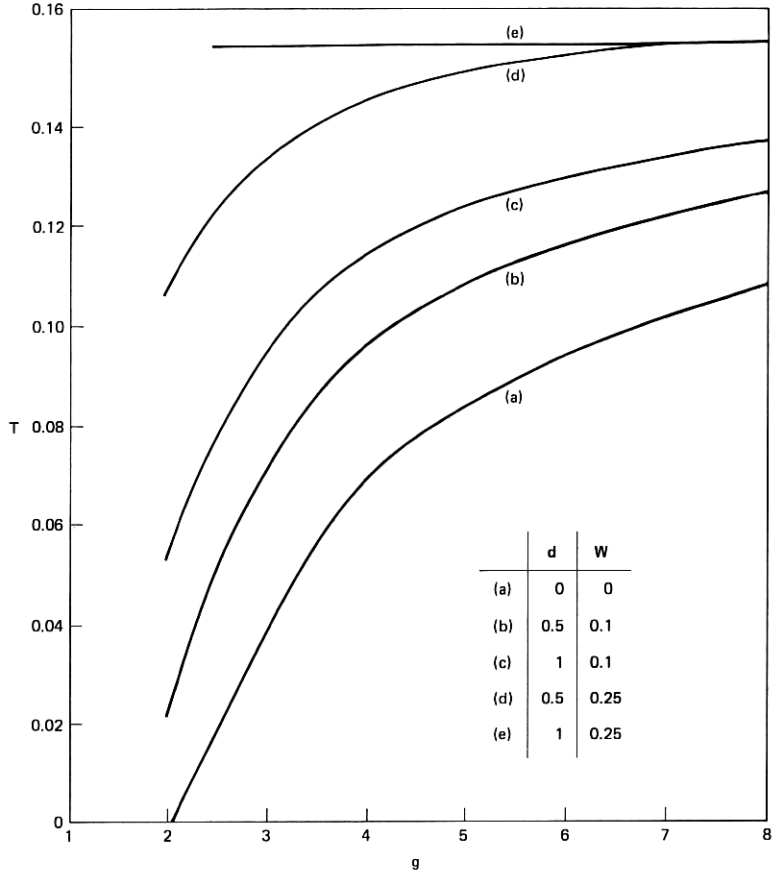


Fig. 7—The maximum delay lag of the LP(11) mode relative to the LP(01) mode plotted vs profile-$g$ for profiles with dips characterized by various depths, $d$, and widths, $w$.

having $g$-profiles with successively smaller $g$-values. Their delay difference curves in Fig. 6 are horizontally displaced from the step-index curves and show that decreasing $g$ increases the LP(01)–LP(11) equalization $V$-number and therefore the fiber diameter corresponding to zero intermodal dispersion. Fiber G-2 had an effective $g \approx 3$ and its equalization $V = 4.25$ number was significantly greater than the effective cut-off $V_{co} \approx 2.9$ number for fabricated step-index fibers.

The (—·—) delay curves in Fig. 6 are computed by $\delta\tau = (L/c)(\bar{\tau}(11) - (\bar{\tau}(01))\Delta n$ from the results in Fig. 1b for fibers with $g = 2.5$ power law profiles which are more optimal for double-mode operation. One of the curves applies to $\Delta = 0.011$ core-cladding refractive-index differences corresponding to the described fabricated profiles. The other curve, with the smaller slope, applies to fibers with $\Delta = 0.001$ that are typical of currently fabricated large-core single-mode fibers. Intermodal dispersion tolerances as a function of fiber profile shape, $V$-number, source wavelength, and spectral bandwidth changes are related to the slope of the delay curves in the vicinity of their zero crossings. The curve in Fig. 6 for $g = 2.5$, $V_0 = 5.5$, $\Delta = 0.001$ indicates that $\delta\tau = 0.114\ \delta V$ ns/Km. Changes in $V$-number are related to changes in wavelength through $\delta V = -V_0\,[(1.28)/\lambda^2]\delta\lambda$. Therefore $\delta\tau = 490\ \delta\lambda$ ps/Km and a pulse broadening requirement of $\delta\tau = 1$ ps/Km limits the source spectral bandwidth to $\delta\lambda < 0.002\ \mu$m which is typical of semiconductor lasers. From the curve in Fig. 3, for $V_0 = 5.5$, $g = 2.5$, and no dip, $\delta g = -6.5\delta V$. Thus changes in profile $g$ are related to changes in wavelength through $\delta g \approx 2.8\delta\lambda$. Therefore a decrease of $\delta g \approx 0.1$ would cause the zero intermodal dispersion wavelength to decrease by $\delta\lambda \approx 0.036\ \mu$m. This wavelength change could be compensated for by decreasing the fiber diameter and therefore the fiber $V$-number.

## IV. CONCLUSIONS

We have reported the first time-domain transmission measurements in double-mode fibers which verify that intermodal dispersion effects can be very small in the 1.3-$\mu$m wavelength region where material dispersion effects are also very small.

One of the graded-index fibers fabricated for this study, with an effective profile $g \approx 3$, had zero intermodal dispersion at $\lambda = 1.24\ \mu$m. This fiber had a $V = 4.25$, which is significantly greater than the effective cut-off $V_{co} \approx 2.9$ for fabricated step-index single-mode fibers. Exact numerical solutions of the scalar wave equations were used to predict that fibers fabricated with $g = 2.5$ power law profiles without a central index dip have zero intermodal dispersion if the fiber $V$-number is 5.5. Additional numerical results showed that profile dips could be partially compensated for by reducing the profile $g$ parameter.

For a system wavelength near $\lambda = 1.3$ $\mu$m, $V = 5.5$ corresponds to a 0.1-percent core-cladding index difference within a core diameter of 35 $\mu$m. This is approximately twice as large as the core diameter of a step-index single-mode fiber designed for the same wavelength.[11]

## REFERENCES


1. K. Okamoto and T. Okoshi, "Analysis of Wave Propagation in Optical Fibers Having Cores with $\alpha$-Power Refractive-Index Distribution and Uniform Cladding," IEEE Trans. on MTT, *24* (1976), pp. 416–421.
2. D. Gloge, "Weakly Guiding Fibers," Appl. Opt., *10* (1971), pp. 2252–2258.
3. L. G. Cohen and Chinlon Lin, "Pulse Delay Measurements in the Zero Material Dispersion Region for Optical Fibers," Appl. Opt., *16* (1977), pp. 3136–3139.
4. D. N. Payne and A. H. Hartog, "Determination of the Wavelength of Zero Material Dispersion in Optical Fibers by Pulse-Delay Measurements," Electron. Lett., *13* (1977), pp. 627–629.
5. G. W. Tasker, W. G. French, J. R. Simpson, P. Kaiser, and H. M. Presby, "Low-Loss Single-Mode Fibers with Different $B_2O_3$—$SiO_2$ Compositions," Appl. Opt., *17* (1978), pp. 1836–1842.
6. L. G. Cohen, W. G. French, Chinlon Lin, and W. L. Mammel, "Propagation Characteristics of Double-Mode Fibers," Tech. Dig. IEEE/OSA Topical Meeting on Optical Fiber Communication, Washington, D.C., March 6–8, 1979.
7. K. Kenichi, Y. Kato, S. Seikai, N. Uchida, and M. Ikida, "Experimental Verification of Modal Dispersion Free Characteristics in a Two-Mode Optical Fiber," IEEE J-QE, *QE-15* (1979), pp. 6–7.
8. L. G. Cohen, W. L. Mammel, and H. M. Presby, "Correlation Between Numerical Predictions and Measurements of Single-Mode Fiber Dispersion Characteristics," Appl. Opt., June 15, 1980.
9. W. L. Mammel and L. G. Cohen, "Prediction of Fiber Transmission Characteristics from Arbitrary Refractive Index Profiles," unpublished work.
10. L. G. Cohen and Chinlon Lin, "A Universal Fiber-Optic (UFO) Measurement System Based on a Near IR Fiber Raman Laser," IEEE J-QE, special issue on Quantum Electronic Devices for Optical-Fiber Communications, *QE-14* (1978), pp. 855–859.
11. N. Kiyoshi, M. Susumu, and T. Ito, "An 800 Mbit/s Optical Transmission Experiment Using a Single-Mode Fiber," IEEE J-QE, *QE-14* (1978) pp. 98–103.